Title

Infrared single spike pulses generation using a short period superconducting tape undulator at APEX

ISBN

9783954501175

Authors

Filippetto, D
Papadopoulos, CF
Penn, G
et al.

Publication Date

2011-12-01

Peer reviewed

INFRARED SINGLE SPIKE PULSES GENERATION USING A SHORT PERIOD SUPERCONDUCTING TAPE UNDULATOR AT APEX*

D. Filippetto†, C.F. Papadopoulos, G. Penn, S. Prestemon, F. Sannibale,
Lawrence Berkeley National Laboratory, 1 Cyclotron Road, Berkeley, CA 94720, USA
C. Pellegrini,
Dept. of Physics, University of California, Los Angeles, CA 90095, USA
M. Yoon,
Dept. of Physics, Postech, Hyoja-dong, Pohang, Gyeongbuk 790-784, Republic of Korea

Abstract

We report on the possibility of constructing an infrared FEL by combining a novel design super-conducting undulator developed at LBNL with the high brightness beam from the APEX injector facility. Calculations show that the resulting FEL is expected to deliver a saturated power of over a MW within a ∼4 m undulator length when operating in Self-Amplified-Spontaneus-Emission mode, with a single-spike of coherent radiation at ∼ 2 μm wavelength. The sub-cm undulator periods, associated with the relatively low energy of the APEX beam (20-25 MeV), forces the FEL to operate in a regime with unusual and interesting characteristics. The alternative option of laser seeding the FEL is also briefly examined, showing the potential to reduce the saturation length even further.

INTRODUCTION

The Advanced Photo-injector EXperiment (APEX) is a compact beam test facility currently under construction at the Lawrence Berkeley National Laboratory (LBNL) [1, 2, 3]. The core of the injector gun is represented by a normal-conducting copper RF cavity resonating in the VHF band (187 MHz), and capable to run in constant wave (CW) mode. Such a cavity combined with a fiber laser and high quantum efficiency (QE) photo-cathodes will allow to generate up to ∼ 1 nC bunches at 1 MHz repetition rate.

The beam energy at the gun will be 0.75 MeV, and a small normal conducting 1.3 GHz pulsed linac will accelerate the beam up to few tens of MeV. Here the repetition rate will be limited to few Hz due to radiation shielding limitations of the Beam Test Facility (BTF), the pre-existing shielded area where APEX is located. Figure 1 shows the CAD view of the APEX injector.

A parallel research is undergoing LBNL to develop a sub-centimeter period. high-temperature super-conducting tape undulator with planar geometry utilizing YBCO material [4, 5]. The technology, if proven, would have a significant impact on the cost of new generation light sources, lowering the beam energy needed to produce a fixed output radiation wavelength.

* Work supported by the Director of the Office of Science of the US Department of Energy under Contract no. DE-AC02-05CH11231

† Dfilippetto@lbl.gov

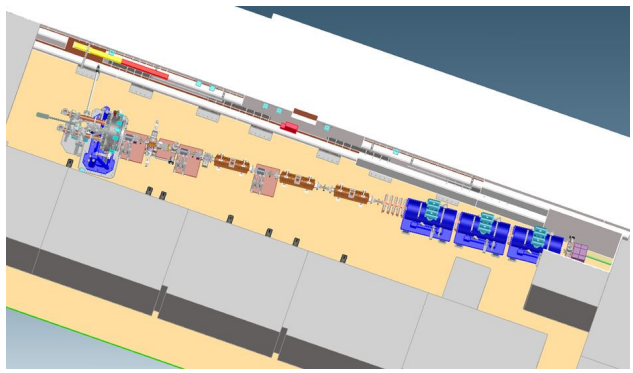

Figure 1: APEX Facility Layout. The electron gun is on the top-left part of the figure while the dark cylinders in the bottom-left are the three undulator cryostats. The total length of the shielded area is about 15 m.

We present a study on the possibility to test such new undulator device by using the APEX beam. Calculations and Genesis simulations [6] show that a fully coherent spike of infrared radiation can be generated if operating the machine at low charge, with a final saturated power in the MW range. Issues related to the matching of a space charge beam into the undulator section have been addressed and some studies have been carried on to model the beam dynamics along the undulator, using PARMELA [7] to take into account both longitudinal and transverse space charge during the transport. This studies do not take into account the FEL process, which develops a microbunching in the beam itself and may worsen the space charge effects. In SASE mode the APEX beam will drive the FEL into saturation in about 4 m. A small seeding of about 10 kW peak power would be enough to decrease the saturation length to less than 1.5 m.

BEAM PARAMETERS

In order to obtain a single spike from the FEL, a electron bunch length of no more than 5-6 coherence lengths σ_c is desired. The coherence length σ_c for the beam parameters reported in Tab. 1, is $\simeq$ 150 fs, compared to the 500 fs rms (root mean square) electron bunch length. The 40 A peak current is reached by rf compression of A 50 pC beam. The consequent loss of beam energy due to the off-crest run of

ISBN 978-3-95450-117-5

Table 1: Parameters of the BTF FEL

Parameter	Value
Radiation wavelength, λ (μm)	1.95
Electron beam energy, E_e (MeV)	23.0
Normalized rms emittance at undulator entrance, ϵ_n (μm)	0.4
Peak electron beam current, I (A)	40
Bunch charge, Q (pC)	50
Rms energy spread at undulator entrance, σ_E (keV)	20
Power gain length (3D), L_g (m)	0.15
FEL parameter (3-D), ρ	4.2×10^{-3}
Rms bunch length, τ_B (fs)	500
Cooperation length, L_c (μm)	41

the first 2 cavities brings the beam energy down to 23 MeV instead of the nominal 30 MeV.

The electron beam emittance much smaller ($\sim$10 times) than the photon emittance for λ_r1.95μm. While a 1D calculation of the FEL gain length L_g would give us L_g=7.5 cm, a 3D calculation using the Ming Xie fitting formula [8] leads to L_g=15 cm, doubling it respect to the one-dimensional case. The efficiency of the coupling between electron and photons is decreased by the photon beam diffraction, with the Raileigh length Z_r=0.2 m not sufficiently bigger than the gain length, and the small electron beam beta function (β=0.75m). A major role is also played by the beam rms energy spread ($\sigma_\gamma/\gamma \sim 10^{-3}$), which is close to the value of the FEL ρ parameter.

SUPER-CONDUCTING TAPE UNDULATOR

A new superconducting undulator is being developed at LBNL, based on the high-temperature superconductor YBCO material ($YBa_2Cu_3O_7$) . The material has a transition temperature of 120 K and critical fields in excess of 100 T. Very high transport current can be maintained in the material if properly manufactured and operated at cryogenic temperatures. The crystal is therefore grown on a appropriate substrate to control the grain orientation, that may limit the maximum current. Tapes with a YBCO core designed for super-conducting magnets applications are commercially available at relatively low cost [4].

The critical transport current J_{sc} in the YBCO layer is a function of temperature, applied magnetic field, and strain. A typical value for commercial tapes is J_{sc}(77 K, 0 T) $\sim$ 30 kA/mm^2; at 4.2 K the value increases by a factor greater than 12.

A flat YBCO tape conductor can be machined with grooves that force the current in a defined path to obtain the desired magnetic field profile. Multiple layers can be super-imposed to yield additional field strength.

A prototype of such an undulator operating at 4.2 K is under development at LBNL, and has been designed to have a 7 mm undulator period, with a 2 mm gap and a field intensity on the axis of $\sim$ 0.92 T sufficient to achieve an undulator parameter $K \sim 0.6$ [5].

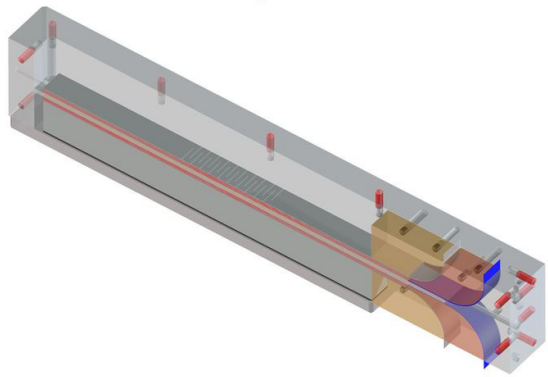

Figure 2: CAD view of the 'cold mass' of the superconducting tape undulator. Not shown in the figure the cryostat that contains the part.

A view of the undulator prototype is shown in Fig. 2. For reference, the width of the part is $\sim$ 4 cm.

BEAM MATCHING AND TRANSPORT

The high current (40 A) and relatively low energy (23 MeV) make the beam space charge forces not negligible after the linac, and the beam matching and the energy spread control not an easy task. Usually the optimization of the beam transport line from the VHF gun to the undulator is done using a combination of the PIC code ASTRA [10] and a genetic optimizer, as described in [9]. In particular, we seek the objectives of low emittance, high peak current and small total rms energy spread. One solution satisfying the conditions described before is shown in Fig. 3. Although this method is well suited for the optimization of beam quality, it is not ideal for finding exact solutions, as required by the matching calculations necessary to match the beam into the undulator. Instead, an alternative approach is taken, and the WARP [11] code is used in envelope mode. The rms quantities out of the linac of a PIC ASTRA simulation are used as input into the envelope code, which is then used to match the β and α functions of the beam. This is done by using 5 quadrupoles in the model, and a conventional simplex optimization algorithm.

Once a solution is found, care is taken to ensure that the ASTRA and WARP envelope codes agree, as shown in Fig. 4.

Non linearities shown in the longitudinal phase space of Fig. 3 develop along the linac, and are strongly dependent from the compression factor one wants to achieve. The slice energy spread (which in the particular case of single spike FEL operation is equal to the full projected energy spread) increases along the line because of longitudinal space charge forces. The simulated energy spread behavior reported in Fig. 5 shows an increase of $\sim$50% along the matching section.

FEL codes usually neglect transverse space charge

ISBN 978-3-95450-117-5

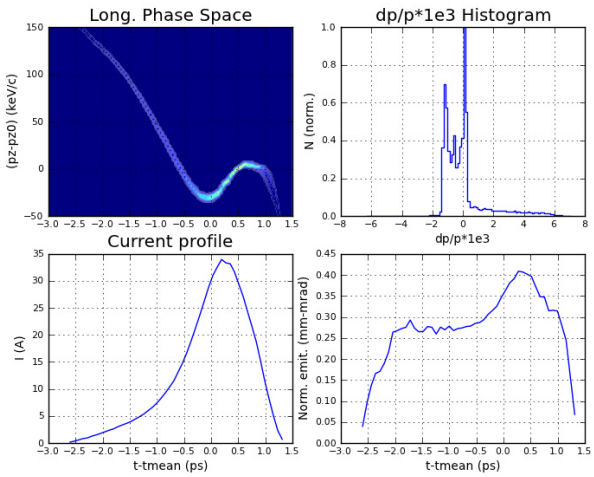

Figure 3: Phase space distribution at the undulator entrance for a possible APEX beam matching the requirements for BTFEL

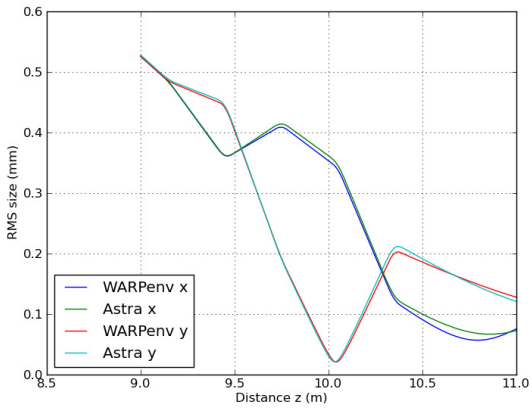

Figure 4: Comparison of WARP envelope model and ASTRA simulation

forces, but in our case they impact both the transverse emittance and the beta functions. In order to estimate such effects, we use PARMELA to simulate the passage of the beam in the undulators. Figure 6 reports the beam beta functions with the presence of transverse space charge. The line was designed to be symmetric by only using linear transform matrices optimization.

Figure 7 reports the transverse emittance variation along the line, in both planes. An increase on both planes is visible, but the reasons are different. In the horizontal plane the undulator does not provide any focusing, and the beam is let free to expand. The space charge term dominates the evolution and increases the emittance. In the second part of the beamline, where focusing is provided, some of the growth is compensated. Vertical emittance growth is very small and is explained by the undulator field non linearities. The small undulator period λ_u is responsible of the strong

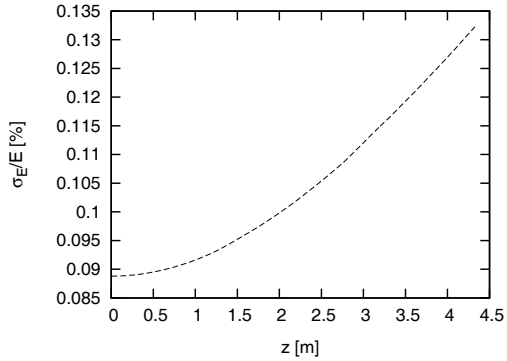

Figure 5: Variation of the rms energy spread (relative) in the undulator in the presence of space charge effect

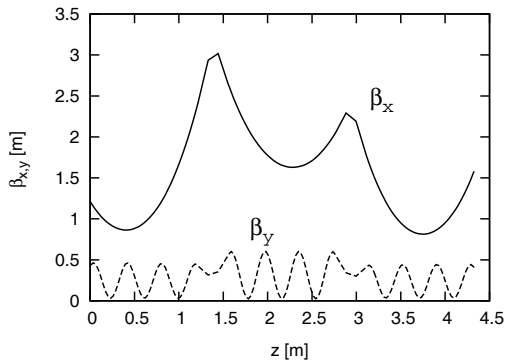

Figure 6: Change in beta functions in the undulator in the presence of space charge effect.

beam focusing in the vertical direction (as can be seen in Fig. 6) . The focusing in the y direction is due to the B_z dependence on the y coordinate as $\sinh(2\pi y/\lambda_u)$. The deviation from linearity starts to be appreciable already at distances from the axis comparable with the beam full width (hundredths of microns).

SIMULATED RESULTS

In order to simulate the FEL performances, both the emittance and the energy spread were increased from the

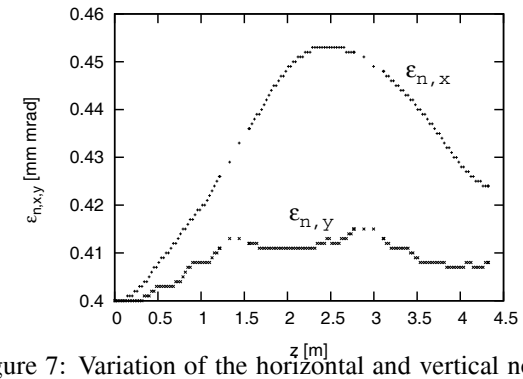

Figure 7: Variation of the horizontal and vertical normalized emittances in the undulator in the presence of space charge effect

ISBN 978-3-95450-117-5

ones found with ASTRA at undulator entrance. A value of 0.5 μm (+25%) for the emittance, and 30 keV (+50%) for the energy spread have been used. Time dependent Genesis simulations have been carried out and the single spike behavior of the FEL pulse has been verified. Figure 8 reports the result of such simulations, for two different emittance values. The pulse reaches the saturation after 4.3 m with a power P$\sim$1.2 MW, and an energy of 0.8μJ. An increase of 15% in energy spread, going from 30 to 35 keV would lead to a power decrease of about 2 orders of magnitude, signature that the regime is much more sensitive to the energy spread that to the emittance.

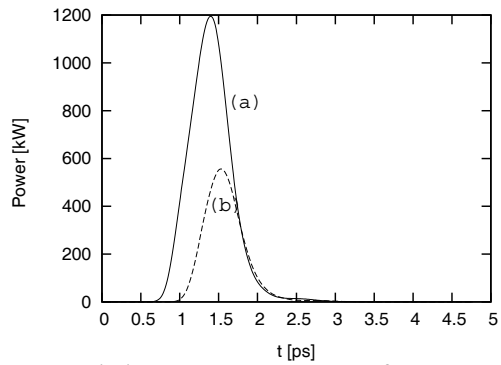

Figure 8: Radiation power at z = 4.3 m from the entrance of the undulator for: (a)$\epsilon_n = 0.5$ μm and $\sigma_E = 30$ keV; (b) $\epsilon_n = 0.6$ μm and $\sigma_E = 30$ keV

Preliminary simulations on the possibility to use a seed to enhance the initial bunching and reach a faster saturation have been carried on. In Fig. 9 the gain curve is reported, showing a saturation distance of 1.2 m. The result has been obtained with a 10 kW-100 fs infrared seed laser.

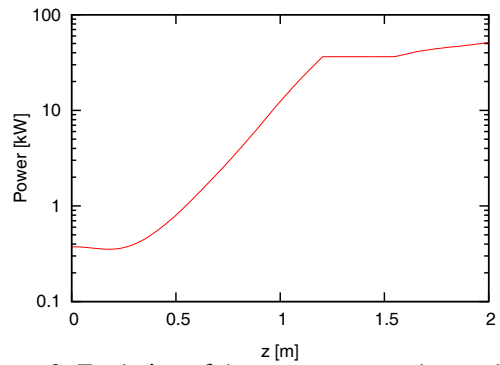

Figure 9: Evolution of the power averaged over slices

CONCLUSIONS

The possibility to test superconducting tape undulators using the APEX beam has been investigated. The low energy of the beam associated with the short period and the small gap of such undulators makes the experiment challenging. Nevertheless It has been demonstrated that, with reasonable beam parameters, a single spike pulse of 0.8μJ can be obtained in about 4 meters. If the FEL is seeded this distance reduces even further to about 1.2 meters. These distances are in agreement with the space available in the cave where the APEX injector is placed.

The sensitivity of the FEL output to the beam parameters has been studied, confirming that the undulator would be a perfect device to measure electron beam slice properties.

REFERENCES

[1] J.Staples, F.Sannibale, S.Virostek, *VHF-band photoinjector*, CBP Tech Note 366, 2006.

[2] K.Baptiste,*et al.*, Nucl. Instrum. Methods Phys. Res., Sect. A **599**, 9 (2009).

[3] F. Sannibale, *et al.*, *Status of the LBNL normal-conducting CW VHF electron photo-gun*, in Proceedings of the 2010 FEL Conference, Malmö, Sweden, August 23-27, 2010.

[4] Peter Lee, `http://www.magnet.fsu.edu/magnettechnology/research/asc/plots.html`.

[5] S. Prestemon, D. Dietderich, A. Madur, S. Marks, R.D. Schlueter, Proceedings of the 2009 Particle Accelerator Conference, Vancouver, BC, Canada, 2009 p. 2438.

[6] S. Reiche, Nucl. Instrum. Methods Phys. Res. Sect. A **429**, 243 (1999).

[7] L. M. Young, PARMELA, LA-UR-96-1835, Revised December 1 (2005).

[8] M. Xie, Nucl. Instrum. Methods Phys. Res. Sect. A **445**, 59 (2000).

[9] C. F. Papadopoulos, D. Filippetto, F. Sannibale, R. Wells. These Proceedings.

[10] Flottmann, K., ASTRA: A space charge tracking algorithm, user's manual available at `http://www.desy.de/~mpyflo/Astra_dokumentation`.

[11] Grote, D. P. and Friedman, A. and Vay, J. L. and Haber, I., Electron Cyclotron Resonance Ion Sources, 749, 55-58, 2005 .

ISBN 978-3-95450-117-5